Electronic and vibronic states of the acceptor–bound-exciton complex (A^0,X) in CdS. II. Determination of the fine structure of the (A^0,X_B) electronic states by high-resolution excitation spectroscopy

J. Gutowski
Institut für Festkörperphysik II, Technische Universität Berlin, Hardenbergstrasse 36, D-1000 Berlin 12, Germany
(Received 11 October 1984)

In a previous paper [R. Baumert, I. Broser, J. Gutowski, and A. Hoffman, Phys. Rev. B 27, 6263 (1983)] it has been shown that high-density, high-resolution excitation spectroscopy gives new information on the electronic and vibronic excited states of the acceptor–bound-exciton complex (A^0,X_A) with two holes from the A valence band in CdS. We now report on corresponding results for the (A^0,X_B) configuration which includes one hole from the second B valence band. This complex is unstable for a very fast $B\rightarrow A$ hole conversion, and therefore gives rise to a set of excitation resonances of the I_1 luminescence arising from the (A^0,X_A) recombination. A detailed theoretical analysis of the energetic structure of the (A^0,X_B) complex including the dependence on the excitation intensity and on an applied magnetic field allows the correct assignment of the excitation resonances to the (A^0,X_B) fine-structure levels originating from the interparticle-exchange interactions. It is shown that the magnetic field is a suitable means of distinguishing the different (A^0,X_B) ground-state levels. The magnetic field also creates allowed transitions which are dipole forbidden in the zero-field case. A self-contained model of the (A^0,X_B) complex thus can be developed, including all symmetry states and yielding adequate values for the exchange energies within the complex.

I. INTRODUCTION

High-density tunable light sources offer extensive possibilities to observe a manifold of excitation and recombination mechanisms of free and bound excitons not known before. In our preceding work[1] we reported on electronic and vibronic excited states of the neutral-acceptor–exciton complex (A^0,X_A) with two holes from the upper A valence band in CdS. They can be observed as excitation resonances of the I_1 luminescence which corresponds to the (A^0,X_A) recombination from the electronic ground state of the complex. Transitions into the excited states are mostly dipole forbidden but visible under dipole-selection-rule breaking conditions as high-density,[1] symmetry disturbance, or phonon participation, e.g., n-LO-phonon Raman processes, where n is the number of the phonons involved.[2]

The occurrence of dipole-forbidden transitions is also known from the donor-bound exciton (D^0,X) in CdS.[3,4] Some excitation resonances of the I_2 luminescence due to the (D^0,X) recombination also observed as absorption lines[5] have been identified as representing quadrupole transitions to excited (D^0,X) states.

Although many luminescence and excitation phenomena in the bound-exciton region of CdS and of other semiconductor compounds have been interpreted as transitions from and into exchange-split ground and excited states of these complexes,[1,2,6–12] up to now there existed considerable problems in the theoretical description of these states and the interactions involved. Mostly, the exciton bound to a neutral impurity, which is a four-particle system, was treated as an analog to the simple diatomic molecules,[13–18] i.e., H_2 or other compounds with one outer shell electron per atom.

These diatomic molecules consist of two heavy and two light particles, i.e., two nuclei and two electrons. Therefore, the calculation can be simplified by a separation of the electronic contribution and the vibronic or rotational contributions as motions of the nuclei. This is not possible in the case of bound excitons[1,13] because the effective masses of the electrons and holes involved are of the same order of magnitude.

In order to compare experimental results and theoretical considerations on bound excitons the observation of systems which show manifold respective transitions is most useful. The acceptor-exciton complex (A^0,X) in CdS fulfills this demand. In 1962 Thomas and Hopfield[13] already described absorption lines due to the two configurations of this complex. One of these configurations is the (A^0,X_A) complex already mentioned above. The second configuration is called (A^0,X_B) and has one hole from the second B valence band lying 16 meV below the A band. The build-up of (A^0,X_B) complexes corresponds to the absorption lines I_{1B} and $I_{1B'}$ (Ref. 13) and the I_1 excitation resonances $I_{1B}^{1,2}$ and $I_{1B'}^{1,2}$ (Ref. 1). These structures represent the splitting of the electronic ground state of the (A^0,X_B) complex by hole-hole and electron-hole exchange interactions between the A and B hole and the electron. Transitions into these split states are observable as excitation resonances of the I_1 luminescence as a rapid $B\rightarrow A$ hole conversion immediately transforms the (A^0,X_B) into an (A^0,X_A) complex.

Although some of the excitation resonances $I_{1B}^{1,2}$ and $I_{1B'}^{1,2}$ are known already,[1,7,9] a correct description of the (A^0,X_B) fine-structure levels could not be given up to now. Mainly this has to be attributed to the lack of high-

resolution measurements with a set of varied parameters. In the following we present experimental results of intensity, polarization, and magnetic-field-dependent measurements at a number of different crystals done in order to get adequate information about the bound-exciton transitions. The results show evidently that the previous assignment of the (A^0,X_B) states to some transitions observed earlier[13] has to be modified. We have been able to improve the theory given in our preceding paper[1] based on Ref. 13 with regard to the new results. For the first time we could calculate the g values of a completed set of (A^0,X_B) states.

II. EXPERIMENTAL TECHNIQUES

The samples used for the measurements were high-quality platelets grown by the Frerich-Warminsky vapor-phase method with a thickness of 30 to 600 μm. The excitation spectra were taken in forward, backward, and right-angle configurations. Tunable dye lasers pumped by an excimer or a N_2 laser served as light sources. The spectral half-width was below 0.02 meV. The spectra were recorded with a double-grating spectrometer (0.75 m). Either a photomultiplier or an optical multichannel analyzer (OMA) were used for the detection. The OMA system is very helpful to divide between luminescence and scattering phenomena and to identify misleading indirect excitation phenomena. The measurements in a magnetic field were performed with a 10-T superconducting split-coil magnet.

III. EXPERIMENTAL RESULTS

A high-resolution analysis of the I_1 luminescence due to the (A^0,X_A) recombination shows that all investigated undoped crystals exhibit a doublet and sometimes a triplet I_1 line structure. It is known that doping of CdS with several chemical elements (mostly alkali metals and halogens) produces additional I_1 luminescence lines or strengthens those of the virgin crystals.[19,20] Some of these lines are separated only by a few hundredths of a nanometer. A spectral analysis is difficult especially if the lines show markedly different intensities. Excitation spectroscopy of the I_1 transitions has to be done with regard to these nearby lines but offers a good possibility to observe even weak I_1 lines lying close to stronger ones, making use of the excitation maxima of the weak lines. In our virgin crystals one always observes two I_1 lines at 2.535 61 eV and 2.535 43 eV, called I_1^a and I_1^b in the following. Due to strong interactions between these nearby transitions excitation resonances of one of them also yield weak resonances of the other and vice versa.

Figure 1 shows a transmission spectrum taken with a high-pressure Hg lamp. The energy region of interest is that of the known[13] absorption lines I_{1B} and $I_{1B'}$ due to the build-up of an (A^0,X_B) complex in two different momenta combinations. However, high resolution yields not only this pair of lines but more structures analogous to the I_1 line doublets or multiplets. In the figure, two sharp absorption lines occur called I_{1B}^1 and I_{1B}^2, on their high-energy side followed by a broader absorption $I_{1B'}^2$. An absorption line $I_{1B'}^1$ corresponding to the I_1 excitation

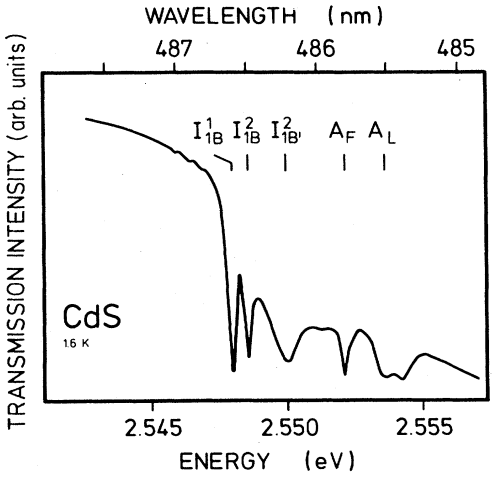

FIG. 1. Transmission spectrum of the free- and bound-exciton energy regime in CdS. Besides the free-exciton absorptions A_F, A_L, three absorption lines I_{1B}^1, I_{1B}^2, and $I_{1B'}^2$ are observable which represent transitions into the (A^0,X_B) ground state split off by the interparticle exchange interactions.

resonance of the same name seems to be unobservable in the absorption spectrum. However, the superposition of the absorption edge of the crystal on the bound-exciton structures can smear a weak line. This is indicated by the fact that $I_{1B'}^2$ exhibits a larger linewidth as in the I_1 excitation spectra (see below). Additionally, it is known that the occurrence of a strong I_{1B}^1 line in absorption as well as in I_1 excitation spectra is not necessarily connected with a strong $I_{1B'}^1$ line. The same holds for the structures I_{1B}^2 and $I_{1B'}^2$.

Further lines in the absorption spectrum are due to the known[21] free-exciton transitions A_F and A_L denoting the triplet and longitudinal free-A-exciton creation. The energies of the absorption lines in comparison with those of the excitation resonances described below are given in Table I.

Figure 2 shows the excitation spectrum of the I_1^a luminescence (2.535 61 eV) taken with laser light polarized in $\mathbf{E}||\mathbf{c}$ direction. Four resonances $I_{1B}^{1,2}$ and $I_{1B'}^{1,2}$ are clearly resolved. The intensity ratio between I_{1B}^1 and I_{1B}^2 changes significantly from crystal to crystal. Thus, these four resonances cannot necessarily be interpreted as transitions into different fine-structure levels of the ground state of the same (A^0,X_B) complex, as done in Ref. 1. All spectra show the sharp resonance A_F and the broader maximum A_L in agreement with the respective absorption lines.

Generally no structures are observed in the I_{1B} spectral region in excitation spectra carefully polarized $\mathbf{E}\perp\mathbf{c}$. The result reported on in Ref. 4, where two resonances were observed in $\mathbf{E}\perp\mathbf{c}$ slightly shifted against those which appeared for $\mathbf{E}||\mathbf{c}$, could not be confirmed. This shift being interpreted in Ref. 4 as the electron-hole-exchange splitting within the (A^0,X_B) ground state may be due to the superposition of a resonant electronic Raman effect at the (A^0,X_B) complex, which can hardly be separated from the

TABLE I. Energies and wavelengths of the absorption lines and excitation resonances due to the creation of an (A^0,X_B) complex in one of its states.

Line	Absorption energy (meV) [wavelength (nm)]	Excitation resonance energy (meV) [wavelength (nm)]
I^1_{1B}	2.547 91 [486.614]	2.547 80 [486.636]
I^2_{1B}	2.548 53 [486.496]	2.548 55 [486.492]
$I^1_{1B'}$		2.549 35 [486.340]
$I^2_{1B'}$	2.549 96 [486.223]	2.550 02 [486.212]

I_1 excitation resonances if a multiplier is the only means of detection. For details see our description of the Raman effect given in paper III of this series (Ref. 22) and another following paper due to the excitation spectroscopy of the I_1—TA-phonon sideband of the I_1 luminescence.[23]

The intensity of all four excitation resonances $I^{1,2}_{1B}$ and $I^{1,2}_{1B'}$ shows a linear increase with the laser light intensity (Fig. 3). A saturation behavior is observed for excitation densities higher than 50 kW cm^{-2}. This is in agreement with the usual intensity dependence of bound-exciton absorption and luminescence in CdS. This is a further hint that all these excitation resonances have to be correlated with transitions into (A^0,X) bound-exciton states. The saturation effect is explained by the limited number of impurities which are able to bind excitons.[1,24]

Performing excitation spectroscopy with a magnetic field applied, one has to attend to the shift of the luminescence line under observation. This shift does not influence the energy position of the excitation resonances but may alter the intensities recorded. Since the characteristics of the I_1 excitation spectra are not influenced by the choice of the I_1 component to be used to record the spectra in a magnetic field, we could follow the component which allowed to observe the most intense excitation structures.

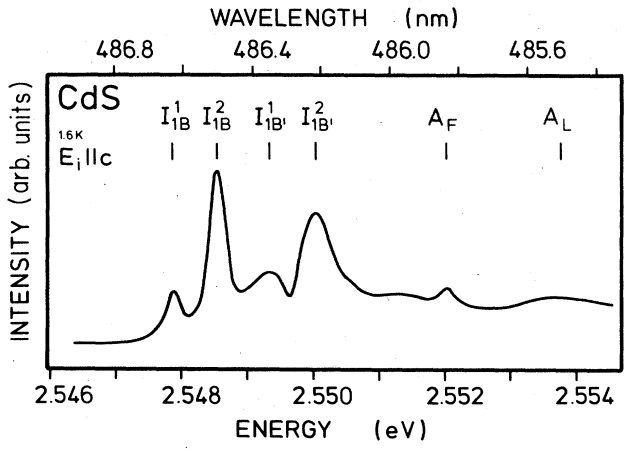

FIG. 2. Excitation spectrum of the I_1^q luminescence taken with incident light polarized $\mathbf{E}||\mathbf{c}$. The excitation resonances correspond to the absorption lines shown in Fig. 1.

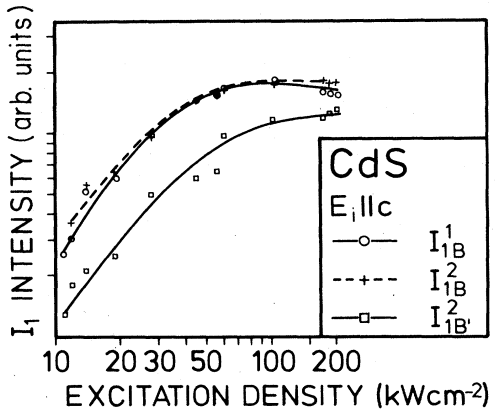

FIG. 3. The I_1 luminescence intensity as a function of the excitation density recorded for the laser energies corresponding to the excitation resonances I^1_{1B}, I^2_{1B}, and $I^2_{1B'}$.

The behavior of the excitation resonances $I^{1,2}_{1B}$ and $I^{1,2}_{1B'}$ in a magnetic field parallel and perpendicular to the c axis is shown in Fig. 4. Obviously I^1_{1B} and I^2_{1B} show the same splitting, and so do $I^1_{1B'}$ and $I^2_{1B'}$. However, in $\mathbf{H}\perp\mathbf{c}$ the high-energy component of $I^1_{1B'}$ which should be weak analogous to that of $I^2_{1B'}$, is not detectable.

In a field oriented $\mathbf{H}\perp\mathbf{c}$, $I^{1,2}_{1B}$ show a threefold splitting. In both cases the middle component being nearly un-

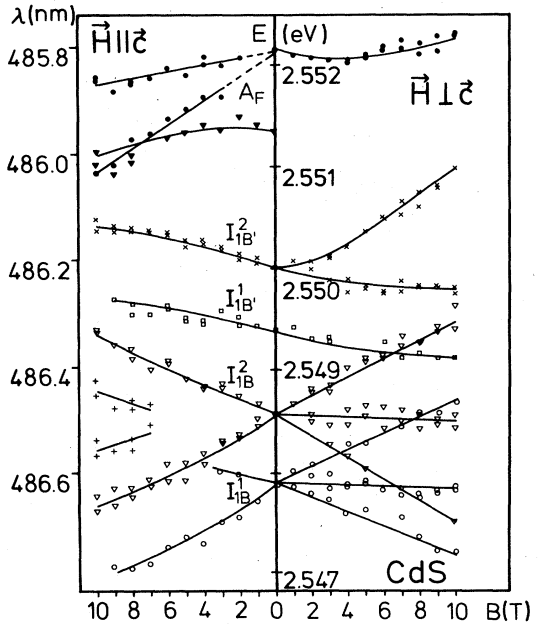

FIG. 4. Splitting of the excitation resonances of the I_1 luminescence as a function of the magnetic field oriented $\mathbf{H}||\mathbf{c}$ and $\mathbf{H}\perp\mathbf{c}$. The excitation resonance A_F corresponds to the free A_F triplet exciton.

changed in energy is the most intense one. The outer two components are nearly equal in intensity. The g value of these outer lines is $g=3.42$ for I^2_{1B} and seems to be slightly smaller for I^1_{1B} although in this case observation was more difficult due to the relatively weak intensities of the outer structures.

For $\mathbf{H}||\mathbf{c}$, I^1_{1B} and I^2_{1B} show exactly the same twofold splitting with $g=2.96$ and with a low-energy component being much stronger than the high-energy one (the behavior of I^1_{1B} was easier to observe in other crystals which presented a more favorable intensity ratio between these two resonances). Additionally, two structures occur between the split components of I^2_{1B} at about 6 T. Their g value is about 1.0, the lower line being the stronger one.

The analysis of the splitting of $I^1_{1B'}$ and $I^2_{1B'}$ is complicated by their larger linewidths (0.5 meV) and lower intensities, which especially is true for $I^1_{1B'}$. Nevertheless, some results have clearly been obtained. Contrary to $I^{1,2}_{1B}$ both lines exhibit distinct diamagnetic shifts in both magnetic field configurations. For $\mathbf{H}\perp\mathbf{c}$, $I^2_{1B'}$ splits into a doublet equal in intensity. The g value amounts to $g=2.05$. Obviously the splitting is superimposed by a nonlinear shift which can be attributed to a diamagnetic shift with $\delta=3.8\ \mu\text{eV T}^{-2}$. We suppose that there also exists a high-energy component of $I^1_{1B'}$ which is not distinctly resolvable because the low-energy line of $I^2_{1B'}$ dominates this spectral region. Some spectra exhibit a slight low-energy shoulder at the lower $I^2_{1B'}$ component, but an exact determination of its position was not possible. Thus energy values due to this shoulder are not included in Fig. 4. For $\mathbf{H}||\mathbf{c}$ both lines $I^1_{1B'}$ and $I^2_{1B'}$ show only one component shifted to higher energies. For both lines, the course of this shift again suggests a superposition of a linear Zeeman effect and a diamagnetic part. The shift with H^2 amounts to $\delta\approx 1.5\ \mu\text{eV T}^{-2}$, whereas a linear portion with $\Delta E=0.47\ \text{meV T}^{-1}$ has to be added. The assumption of a very weak and therefore not observable low-energy component fits to respective results in absorption[5] and to the theory (Sec. IV). A g value of 1.6 to 1.9 would follow from the suggestion of a twofold splitting, assuming the observable line to be the high-energy component.

In agreement with known results,[21] A_F shows no splitting in $\mathbf{H}\perp\mathbf{c}$, which has to be expected for this state with Γ_6 symmetry. For $\mathbf{H}||\mathbf{c}$ a twofold splitting occurs connected with an energy shift. Additionally, in some spectra a new structure between A_F and $I^2_{1B'}$ appears, showing no split off but a distinct diamagnetic shift.

The g values, diamagnetic shifts, and line intensities are given in summary in Table II.

IV. THEORY AND DISCUSSION

A. Group-theoretical results

The electronic ground state of the (A^0,X_B) complex involves, apart from the acceptor ion, one hole from the B valence band, one hold from the A valence band, and one

TABLE II. Splitting, g values, diamagnetic shifts, and intensities of the I_1 excitation resonances.

Line	$\mathbf{H}\perp\mathbf{c}$	$\mathbf{H}\|\|\mathbf{c}$
I^1_{1B}	Threefold splitting $g=3.2$ Middle line strong, outer lines equal in strength	Twofold splitting $g=2.96$ Low-energy line strong $\delta=1.6\ \mu\text{eV T}^{-2}$
I^2_{1B}	Threefold splitting $g=3.42$ Middle line strong, outer lines equal	Twofold splitting $g=2.96$ Low-energy line strong $\delta=1.6\ \mu\text{eV T}^{-2}$ More than 5 T: two inner components $g\approx 1.0$ Low-energy line strong
$I^1_{1B'}$	Twofold (?) splitting Only low-energy component Probably like $I^2_{1B'}$	Twofold (?) splitting Only high-energy component $g\approx 1.9$ $\delta\approx 1.5\ \mu\text{eV T}^{-2}$
$I^2_{1B'}$	Twofold splitting $g=2.05$ both lines equal in strength $\delta=3.8\ \mu\text{eV T}^{-2}$	Twofold (?) splitting Only high-energy component $g\approx 1.9$ $\delta\approx 1.5\ \mu\text{eV T}^{-2}$
A_F	No splitting $\delta=3.25\ \mu\text{eV T}^{-2}$	Twofold splitting $g=1.46$ $\delta=7.6\ \mu\text{eV T}^{-2}$
New structure		No splitting $\delta=2.76\ \mu\text{eV T}^{-2}$

electron from the conduction band. This four-particle system underlies hole-hole and electron-hole exchange interactions. Therefore the electronic ground state is split off into four terms with different exchange energies due to the different spin and angular momenta adjustments of the particles. This was discussed in detail in our preceding paper (Ref. 1), so only the results are given here.

As Thomas and Hopfield[13] pointed out in the case of weakly bound states at an impurity and for energy bands near $\mathbf{k}=\mathbf{0}$ it is not necessary to describe the states as belonging to the point group of the impurity. They also can be treated as states within the point group of the crystal. Thus the particles have the symmetry representations of the bands they stem from. In the (A^0,X_B) complex in CdS with the point group C_{6v}^+, the A hole is characterized by the representation Γ_9 of the A valence band, while the B hole and the electron have the representation Γ_7, similar to the B valence band and the conduction band. Therefore, the (A^0,X_B) states are determined by the group-theoretical product of the representations of the particles:

$$\Gamma_7\times(\Gamma_7\times\Gamma_9)=\Gamma_7+\Gamma_8+2\Gamma_9\ . \tag{1}$$

The group-theoretical notations and equations are used following Koster *et al.*[25] If both holes have their spins parallel, the coupling of the electron to the two holes will result in two states $\Gamma_8(J_z=\frac{5}{2})$ and $\Gamma_9(J_z=\frac{3}{2})$. In the case of antiparallel hole spins one finds $\Gamma_7(J_z=\frac{1}{2})$ and $\Gamma_9(J_z=\frac{3}{2})$. The transition to the impurity point group C_{3v}^+ in CdS does not affect the following results. For that reason the (A^0,X_B) states also may be treated in C_{3v}^+. The representations Γ_7 and Γ_8 in C_{6v}^+ are compatible with Γ_4 in C_{3v}^+, and Γ_9 with $\Gamma_5\oplus\Gamma_6$, which is a degenerate Kramers doublet. A magnetic field oriented $\mathbf{H}\perp\mathbf{c}$ reduces the symmetry from C_{3v}^+ (C_{6v}^+) into C_S. A field $\mathbf{H}\|\mathbf{c}$ results in a reduction from C_{3v}^+ (C_{6v}^+) into C_3^+ (C_6^+). Figure 5 shows the splitting and the representations of the states in a magnetic field $\mathbf{H}\perp\mathbf{c}$ and $\mathbf{H}\|\mathbf{c}$. (The term sequence and the energy distances cannot be determined by group theory. This has to be done using additional information given by the analysis of the interparticle interactions and of the perturbation of the system caused by a magnetic field. This will be treated in Sec. IV B.) The starting point is the impurity point group C_{3v}^+. In parenthesis the representations are given for the group C_{6v}^+. The neutral acceptor A^0 with the representation $\Gamma_5\oplus\Gamma_6$ (Γ_9) is the final state of all transitions from bound-exciton levels. To decide which transitions are dipole allowed for a polarization $\mathbf{E}\perp\mathbf{c}$ or $\mathbf{E}\|\mathbf{c}$ one has to determine the group-theoretical products of the transitions. Table III is a compatibility table for the representations of interest. The electric dipole operator for the case $\mathbf{E}\|\mathbf{c}$ in C_{3v}^+ (C_{6v}^+) has

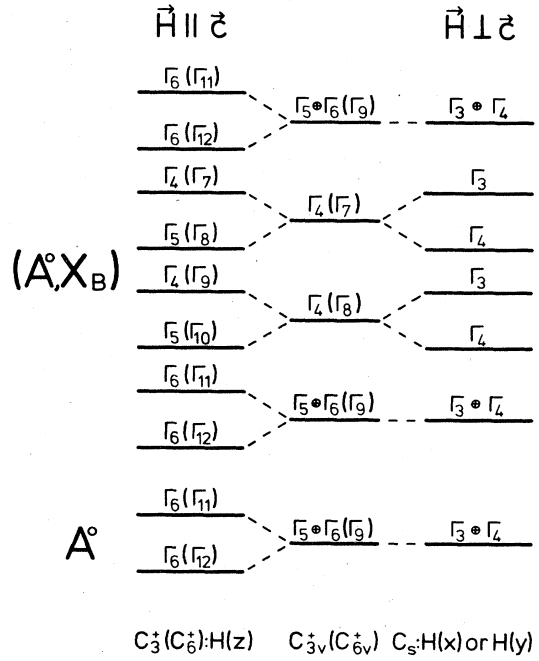

FIG. 5. Term scheme of the (A^0,X_B) complex's ground state split off by hole-hole and electron-hole exchange interaction. The scheme is given for a zero-field $\mathbf{H}=\mathbf{0}$, for $\mathbf{H}\|\mathbf{c}$, and for $\mathbf{H}\perp\mathbf{c}$. Below, the point-symmetry group is indicated for the zero-field case as well as for the case of the different magnetic fields applied, which reduce the crystal symmetry in a characteristic manner (see text). The representations noticed for each electronic state of the (A^0,X_B) complex belong to the respective symmetry group given below. To present an easily surveyed picture the term sequence has been drawn without regard to the real energy distances determined by the experimental results. As shown in Secs. IV B and IV C, the upper Γ_4 and $\Gamma_5\oplus\Gamma_6$ states exhibit a very small energy distance ($<40\ \mu$eV), and so do the lower Γ_4 and $\Gamma_5\oplus\Gamma_6$ states, while the distance between these two couples of states amounts to 1.3 meV. Thus the magnetic field produces level crossings between those components which originate from two nearby states (see Sec. IV C).

the representation Γ_1, for $\mathbf{E}\perp\mathbf{c}$ Γ_3 (Γ_5). While Γ_1 remains the representation valid for C_3^+ (C_6^+) and C_S, that of the operator $\mathbf{E}\perp\mathbf{c}$ is transferred into $\Gamma_2+\Gamma_3$ ($\Gamma_5+\Gamma_6$) in C_3^+ (C_6^+) and into $\Gamma_1+\Gamma_2$ in C_S.

A transition is dipole allowed if the product $\Gamma_i\times\Gamma_{\rm op}$ includes Γ_f, with Γ_i as representation of the initial state, $\Gamma_{\rm op}$ as that of the dipole operator, and Γ_f as that of the final state. Table IV gives a survey of the transitions allowed without a magnetic field and with a magnetic field

TABLE III. Compatibility table for the representations of interest in the different point groups.

	$\mathbf{E}\|\mathbf{c}$	$\mathbf{E}\perp\mathbf{c}$	C_{6v}^+: Γ_7	C_{6v}^+: Γ_8	C_{6v}^+: Γ_9
$\mathbf{H}=\mathbf{0}$: C_{6v}^+	Γ_1	Γ_5	Γ_7	Γ_8	Γ_9
$\mathbf{H}=\mathbf{0}$: C_{3v}^+	Γ_1	Γ_3	Γ_4	Γ_4	$\Gamma_5\oplus\Gamma_6$
$\mathbf{H}(z)$: C_3^+ (C_6^+)	Γ_1 (Γ_1)	$\Gamma_2+\Gamma_3$ ($\Gamma_5+\Gamma_6$)	$\Gamma_4+\Gamma_5$ ($\Gamma_7+\Gamma_8$)	$\Gamma_4+\Gamma_5$ ($\Gamma_9+\Gamma_{10}$)	$\Gamma_6+\Gamma_6$ ($\Gamma_{11}+\Gamma_{12}$)
$\mathbf{H}(x)$: C_S	Γ_1	$\Gamma_1+\Gamma_2$	$\Gamma_3+\Gamma_4$	$\Gamma_3+\Gamma_4$	$\Gamma_3+\Gamma_4$

TABLE IV. Allowed dipole transitions between the (A^0,X_B) and the A^0 states with $\mathbf{H}=0$, $\mathbf{H}\|\mathbf{c}$ [$\mathbf{H}(z)$], and $\mathbf{H}\perp\mathbf{c}$ [$\mathbf{H}(x)$]. The first column gives the representations of the Γ_7 spin state of the (A^0,X_B) for the three cases $\mathbf{H}=0$, $\mathbf{H}\|\mathbf{c}$, $\mathbf{H}\perp\mathbf{c}$, the second column those of the Γ_8 spin state and the third column those of the two Γ_9 spin states. The first line has to be read as the dipole-allowed transitions in the case $\mathbf{H}=0$, the second line presents those under $\mathbf{H}\|\mathbf{c}$ and the third line those under $\mathbf{H}\perp\mathbf{c}$.

A^0 \ (A^0,X_B) Γ_i / Γ_f		Γ_4 (Γ_7)	Γ_4 (Γ_8)	$\Gamma_5\oplus\Gamma_6$ (Γ_9)
$\mathbf{H}=0$ C_{3v}^+ (C_{6v}^+):	$\Gamma_5\oplus\Gamma_6$ (Γ_9)	$\mathbf{E}\perp\mathbf{c}$	$\mathbf{E}\perp\mathbf{c}$	$\mathbf{E}\|\mathbf{c}$
$\mathbf{H}(z)$ C_3^+ (C_6^+):	$\Gamma_6+\Gamma_6$ ($\Gamma_{11}+\Gamma_{12}$)	$\mathbf{E}\perp\mathbf{c}$	$\mathbf{E}\perp\mathbf{c}$	$\mathbf{E}\|\mathbf{c}$
$\mathbf{H}(x)$ C_S:	Γ_3, Γ_4	$\mathbf{E}\|\mathbf{c}$ and $\mathbf{E}\perp\mathbf{c}$	$\mathbf{E}\|\mathbf{c}$ and $\mathbf{E}\perp\mathbf{c}$	$\mathbf{E}\|\mathbf{c}$ and $\mathbf{E}\perp\mathbf{c}$
$\mathbf{H}(z)$ C_3^+ (C_6^+):	Γ_6 (Γ_{11}), Γ_6 (Γ_{12})	$\mathbf{E}\perp\mathbf{c}$	$\mathbf{E}\perp\mathbf{c}$	$\mathbf{E}\|\mathbf{c}$
$\mathbf{H}(x)$ C_S:	Γ_3, Γ_4	$\mathbf{E}\|\mathbf{c}$ and $\mathbf{E}\perp\mathbf{c}$	$\mathbf{E}\|\mathbf{c}$ and $\mathbf{E}\perp\mathbf{c}$	$\mathbf{E}\|\mathbf{c}$ and $\mathbf{E}\perp\mathbf{c}$

applied parallel and perpendicular to the c axis. A field $\mathbf{H}\|\mathbf{c}$ does not change the situation compared to the zero-field case. Only transitions polarized $\mathbf{E}\perp\mathbf{c}$ are possible between the A^0 final state and those terms which originate from the two Γ_4 (Γ_7) and Γ_4 (Γ_8) configurations of the (A^0,X_B) complex. Transitions between the terms arisen from the two $\Gamma_5\oplus\Gamma_6$ (Γ_9) levels and the A^0 remain possible only for $\mathbf{E}\|\mathbf{c}$.

In contrast, a magnetic field $\mathbf{H}\perp\mathbf{c}$ drastically reduces the symmetry to C_S. Transitions between all states of the (A^0,X_B) complex and the A^0 final state become possible in both polarizations.

B. Energies of the (A^0,X_B) states in a magnetic field

While group-theoretical considerations enable one to describe the symmetry states of the (A^0,X_B) complex and the possible lifting of their degeneracy by additional fields, nothing can be said about the term sequence and energy distances without and with a magnetic field applied. So one has to use some theoretical results which describe the influence of the magnetic field on the spin and angular momenta configurations of the (A^0,X_B) levels.

First of all, Thomas and Hopfield[13] tried to calculate the energy distance between the four (A^0,X_B) levels under zero-field conditions. According to their model, the exchange interaction between the A and B valence-band holes yields two states Γ_5 and Γ_6 with a distance of $0.4P(0)$ eV. $P(0)$ is the probability that the two holes in a bound state lie in the same unit cell. Thomas and Hopfield[13] interpreted the distance between the observed absorption lines I_{1B} and $I_{1B'}$ as being the energy difference between these two hole states. Thus the experimentally determined energy distance between the states amounts to 1.3×10^{-3} eV. This yields a $P(0)$ of about 3×10^{-3}. The exchange interaction between the holes and the additional electron gives rise to a further twofold split off of the Γ_5 as well as of the Γ_6 level. This coincides with the finding of the four states $\Gamma_7+\Gamma_9$ and $\Gamma_8+\Gamma_9$ using the group theory (Sec. IV A). The energy distances between Γ_7 and Γ_9 on the one hand and Γ_8 and Γ_9 on the other hand were estimated to be $0.04P'(0)$ eV.[13] $P'(0)$ is the possibility that the electron and the hole lie in the same unit cell. However, there has been no experimental evidence of the electron-hole exchange interaction. Thomas and Hopfield[13] observed a weak absorption structure in $\mathbf{E}\perp\mathbf{c}$ polarized spectra shifted by 0.27 meV against I_{1B}. The interpretation of this line to be the transition into the Γ_8 state as the second level created from Γ_6 by the additional electron-hole exchange interaction led to the assumption of $P'(0)=10^{-2}$. This not only contradicts the fact that in case of an electron bound to a hydrogenic donor $P'(0)$ does not exceed 10^{-3} but also the knowledge that the electron is the lightest particle in the (A^0,X_B) complex with the greatest distance to the center.[26,27] Therefore the assumption by Thomas and Hopfield does not seem to be realistic. $P'(0)$ should be smaller than 10^{-3}, which results in a value of at most 40 μeV for the electron-hole—exchange split off.

Now, on the basis of these considerations, the influence of a magnetic field has to be treated. The four-particle system (A^0,X_B) can be looked upon as an analog to a diatomic molecule. The application of a magnetic field results in a diamagnetic shift of the terms proportional to H^2 and in a linear Zeeman split off, provided that the terms do not strongly mix.[28] The diamagnetic shift of excitonic complexes is proportional to $(e^2/2\mu c^2)\mathbf{A}^2$ with $\nabla\times\mathbf{A}=\mathbf{H}$ and μ as the reduced mass of the exciton. Since μ is small compared to m_0 in CdS, the diamagnetic shift is expected to be clearly noticeable. However, the diamagnetic shift is not very helpful for the identification of transitions, and therefore shall not be discussed here in detail. The Zeeman effect can be treated as a perturbation of the zero-field case. From the wave functions and the Clebsch-Gordan coefficients (Koster *et al.*[25]) of the states Γ_4 (Γ_7), Γ_4 (Γ_8), and $\Gamma_5\oplus\Gamma_6$ (Γ_9) in C_{6v}^+ (the change over to C_{3v}^+ yields corresponding relations) and the operator of the magnetic field $\hat{H}=g\mu_B H(\hat{L}+2\hat{S})$ the following Zeeman matrices result:

$$\langle\hat{H}(\Gamma_7)\rangle=\langle\hat{H}(\Gamma_8)\rangle=(g\mu_B H)^2\begin{bmatrix}\cos\theta & \frac{1-i}{2}\sin\theta\\ \frac{1+i}{2}\sin\theta & -\cos\theta\end{bmatrix}, \tag{2}$$

$$\langle\hat{H}(\Gamma_9)\rangle=(g\mu_B H)^2\begin{bmatrix}\cos\theta & 0\\ 0 & -\cos\theta\end{bmatrix}. \tag{3}$$

A magnetic field $\mathbf{H}\perp\mathbf{c}$ mixes the states Γ_7 and Γ_9 as well as Γ_8 and Γ_9. This is described by the matrix

$$\langle \hat{H}(\Gamma_7\oplus\Gamma_9)\rangle = \langle \hat{H}(\Gamma_8\oplus\Gamma_9)\rangle = (g\mu_B H)^2 \begin{pmatrix} \cos\theta & \frac{1-i}{2}\sin\theta & 0 \\ \frac{1+i}{2}\sin\theta & 0 & \frac{1-i}{2}\sin\theta \\ 0 & \frac{1+i}{2}\sin\theta & -\cos\theta \end{pmatrix} . \tag{4}$$

Up to now the anisotropy of the g value has not been included. To insert the anisotropic g values the matrices have to be changed in the following manner:

$$\langle \hat{H}(\Gamma_8)\rangle_{\text{an}} = (\mu_B H)^2 \begin{pmatrix} g_{1,\parallel}\cos\theta & g_{1,\perp}\frac{1-i}{2}\sin\theta \\ g_{1,\perp}\frac{1-i}{2}\sin\theta & -g_{1,\parallel}\cos\theta \end{pmatrix} , \tag{5}$$

where the subscript an marks the anisotropic case. The eigenvalues are

$$E(\Gamma_8) = \pm\mu_B H(g_{1,\parallel}^2\cos^2\theta + g_{1,\perp}^2\sin^2\theta)^{1/2} = \mu_B H g_{1,\text{eff}} , \tag{6}$$

where the expression in parenthesis is defined as $g_{1,\text{eff}}$. For $\langle \hat{H}(\Gamma_7)\rangle$ and $E(\Gamma_7)$ one has to insert $g'_{1,\parallel}$ and $g'_{1,\perp}$. In the case of the Γ_9 states only a "parallel" g value enters into the equation:

$$\langle \hat{H}(\Gamma_9)\rangle_{\text{an}} = (\mu_B H)^2 \begin{pmatrix} g_{2,\parallel}\cos\theta & 0 \\ 0 & -ig_{2,\parallel}\cos\theta \end{pmatrix} . \tag{7}$$

This results in the eigenvalues

$$E(\Gamma_9) = \mu_B H g_{2,\parallel}\cos\theta . \tag{8}$$

The matrix (4) for $\mathbf{H}\perp\mathbf{c}$ has to be changed as follows:

$$\langle \hat{H}(\Gamma_8\oplus\Gamma_9)\rangle_{\text{an}} = (\mu_B H)^2 \begin{pmatrix} g_{3,\parallel}\cos\theta & g_{3,\perp}\frac{1-i}{2}\sin\theta & 0 \\ g_{3,\perp}\frac{1-i}{2}\sin\theta & 0 & g_{3,\perp}\frac{1-i}{2}\sin\theta \\ 0 & g_{3,\perp}\frac{1+i}{2}\sin\theta & -g_{3,\parallel}\cos\theta \end{pmatrix} . \tag{9}$$

From (9), three eigenvalues are calculated:

$$\begin{aligned} E(\Gamma_8\oplus\Gamma_9) &= 0 , \quad \pm\mu_B H(g_{3,\parallel}^2\cos^2\theta + g_{3,\perp}^2\sin^2\theta)^{1/2} \\ &= 0 , \quad \pm\mu_B H g_{3,\text{eff}} , \end{aligned} \tag{10}$$

where the expression in parentheses is defined as $g_{3,\text{eff}}$. Within the eigenvalues $E(\Gamma_7\oplus\Gamma_9)$ there occur $g'_{3,\parallel}$ and $g'_{3,\perp}$ and therefore $g'_{3,\text{eff}}$ in Eqs. (9) and (10).

The conclusions drawn from these results are as follows.

(i) A magnetic field $\mathbf{H}\perp\mathbf{c}$ is not able to lift the degeneracy of the Γ_9 ($\Gamma_5\oplus\Gamma_6$) states of C_{6v}^+ (C_{3v}^+). The representations $\Gamma_3+\Gamma_4$ (see Fig. 5) in C_S remain a Kramers doublet.

(ii) The degeneracy of Γ_8 (Γ_4) and Γ_7 (Γ_4) is lifted by a field $\mathbf{H}\perp\mathbf{c}$.

(iii) Due to the mixing of the states in the case $\mathbf{H}\perp\mathbf{c}$, one has to expect a threefold splitting following Eq. (10).

(iv) In the case $\mathbf{H}\parallel\mathbf{c}$ the degeneracy of all (A^0,X_B) states is lifted. This results in a twofold splitting of all lines.

Figure 5 shows the results with regard to the group-theoretical considerations as well as to the matrix calculations given above. The dipole transitions within this term scheme are given by the use of Table IV. To determine the theoretical values of the $g_{i,\parallel}$ and $g_{i,\perp}$ one has to make use of the molecular analogy. In the case of parallel hole spins and antiparallel electron spin (i.e., the lower Γ_9 state), with regard to Ref. 28 one obtains a $g_{2,\parallel}$ which is (in accordance with Ref. 13)

$$g_{2,\parallel} = g_{hA} + g_{hB\parallel} - g_e . \tag{11}$$

g_{hA} is the g value of the A valence-band hole. Here the sign $\parallel$ is dispensable because the perpendicular component plays no role due to the complete anisotropy of the A hole splitting.[13] $g_{hB\parallel}$ is the parallel part of the B hole g value, g_e the isotropic electron g value. $g_{hB\perp}$ does not appear because of the $\cos\theta$ factor of the Γ_9 state. The configuration which corresponds to antiparallel hole spins and the electron spin being parallel to that of the B hole is described by

$$g'_{2,\parallel} = g_{hA} - g_{hB\parallel} - g_e . \tag{12}$$

C. Application to the I_{1B} transitions

As pointed out at the beginning of Sec. III all investigated crystals show at least two I_1 emission structures with intensity ratios varying from crystal to crystal. Each of the lines exhibit distinct excitation resonances which make possible a clear distinction between the nearby luminescence transitions. The observed luminescence lines called I_1^a and I_1^b have the energies 2.535 61 eV (488.975 nm) and 2.535 43 eV (489.010 nm). The line I_1^a coincides with those discussed in literature as due to an acceptor built by a Cd-vacancy—Al complex[19] $(V_{Cd}{}^{2-}Al_{Cd}{}^{+})^{-}$ or by $Li_{Cd}{}^{-}$.[20] The I_1^b line is identical in energy to an emission line identified to include a $(V_{Cd}{}^{2-}Cl_S{}^{+})^{-}$ acceptor.[19] Although all four excitation resonances $I_{1B}^{1,2}$ and $I_{1B'}^{1,2}$ appear in the excitation spectra of both I_1 lines, it was pointed out in Sec. III that I_{1B}^1 and $I_{1B'}^1$ are identified as being resonances of the 2.535 61-eV—I_1^a line whereas I_{1B}^2 and $I_{1B'}^2$ belong to the 2.535 43-eV—I_1^b line. I_{1B}^1 as a sharp line and $I_{1B'}^1$ as a broad one resemble the known $I_{1B}/I_{1B'}$ absorption doublet,[13] and so do I_{1B}^2 as a sharp and $I_{1B'}^2$ as a broad line. It is known from absorption, emission,[13] and excitation spectroscopy[1] that the creation of an (A^0,X_B) complex is followed by a rapid conversion of the B hole into an A hole and therefore by the transition of the whole complex into an (A^0X_A) configuration which recombines producing the I_1 luminescence. Therefore we have to assume that I_{1B}^1 and $I_{1B'}^1$ are transitions into the upper and the lower Γ_9 level (Fig. 5) of the (A_a^0,X_B) complex where A_a^0 may be the $(V_{Cd}{}^{2-}Al_{Cd}{}^{+})^{-}$ or $Li_{Cd}{}^{-}$ acceptor. I_{1B}^2 and $I_{1B'}^2$ then belong to the Γ_9 levels of the (A_b^0,X_B) with an acceptor A_b^0 possibly being the $(V_{Cd}{}^{2-}Cl_S{}^{+})^{-}$ acceptor.

The binding energies of the complexes show an interesting behavior. While the (A_a^0,X_A) complex due to the I_1^a line has a binding energy of 18.09 meV for the exciton at the acceptor [taking the energy of the free A exciton as 2.5537 eV (Refs. 21 and 29)], the (A_b^0,X_A) complex due to the I_1^b is more strongly bound with 18.27 meV. In contrast to the (A^0,X_A) levels, the (A^0,X_B) states show an inverted behavior of the binding energies. The (A_a^0,X_B) complex exhibits binding energies of 20.90 meV for the lower Γ_9 level due to the I_{1B}^1 transition and 19.35 meV for the upper Γ_9 level due to the $I_{1B'}^1$ [taking the energy of the free B exciton as 2.5687 eV (Ref. 21)]. Here (A_b^0,X_B) is the complex which is more weakly bound by 20.15 meV for the lower Γ_9 state (I_{1B}^2) and by 18.68 meV for the upper Γ_9 state $(I_{1B'}^2)$.

The binding energy of an acceptor-exciton complex sensitively depends on the interparticle distances, i.e., the amount of the exchange interactions.[16,18] Therefore, it is concluded that in the (A_a^0,X_A) complex the electron is further away from the center than in the (A_b^0,X_A) complex, whereas the opposite has to be assumed for the B hole complexes (A_a^0,X_B) and (A_b^0,X_B). This phenomenon is not explainable in the framework of the models used up to now for the calculation of bound-exciton binding energies. The binding energy mainly depends on the mass ratio $\sigma=m_e^*/m_h^*$ of the effective masses of the electrons and holes involved. Moreover, it is known that the binding energy depends on the Rydberg energy of the impurity.[16–18,30] Therefore the impurity Bohr radii of chemically different acceptor atoms or acceptor complexes enter into the calculations of the binding energy. But in theory this influence is monotonous, i.e., the exciton binding energy increases and the interparticle distances decrease for increasing impurity Rydberg values and decreasing impurity Bohr radii. This was assumed to be valid for all values of $\sigma=m_e^*/m_h^*$.[18,30] However, this is not consistent with our experimental results which demand that the exciton should be more weakly bound within an (A^0,X_A) complex but more strongly bound within an (A^0,X_B) complex if the acceptor A_b^0 is replaced by an A_a^0 acceptor, i.e., a $(V_{Cd}{}^{2-}Cl_S{}^{+})^{-}$ acceptor is replaced by a $(V_{Cd}{}^{2-}Al_{Cd}{}^{+})^{-}$ or a $Li_{Cd}{}^{+}$ acceptor provided these are really the acceptors A_b^0 and A_a^0, respectively. The interparticle distances and the screening of the repulsive interaction between the acceptor ion and the electron caused by the two holes seem to depend not only on the Coulomb and exchange interactions between these particles but also on the nature of the acceptor, i.e., its spacial structure and its inner electron shell.

The intensity dependence (Fig. 3) of all $I_{1B}^{1,2}$ and $I_{1B'}^{1,2}$ resonances clearly shows that these resonances have to be assigned to transitions into bound-exciton states. They show the same behavior as the I_1 luminescence itself including a high-density saturation effect due to the limited number of acceptors.

Zeeman measurements of the absorption lines I_{1B} and $I_{1B'}$ only have been performed by Thomas and Hopfield[13] in 1962 and by Roussel from our institute in 1979.[5] Thomas and Hopfield did not observe enough lines and could not use fields higher than 3.1 T. No consistent explanation of the results has been given up to now. Our model, however, is also able to explain the results of Ref. 5.

In the Zeeman measurements of the I_1 excitation spectra the resonances I_{1B}^1 and I_{1B}^2 show a nearly identical splitting. The same holds for $1_{1B'}^1$ and $I_{1B'}^2$. This underlines the interpretation of I_{1B}^1 and $I_{1B'}^1$ as transitions within the (A_a^0,X_B) complex and I_{1B}^2 and $I_{1B'}^2$ as those within the (A_b^0,X_B) complex.

1. *The transitions I_{1B}^1 and I_{1B}^2*

(a) $\mathbf{H}\perp\mathbf{c}$. As indicated above, the absorption lines I_{1B} and $I_{1B'}$ up to now have been interpreted as transitions into the two Γ_9 levels of the (A^0,X_B) complex[13] (see Fig. 5). Transitions into the Γ_8 and Γ_7 levels were expected to lie some tenth of a meV away from I_{1B} and $I_{1B'}$. Except for two lines observed under probably misleading conditions[4,13] and interpreted as one of these additional transitions, no experimental evidence of these lines could be given up to now. The Zeeman measurements of the excitation resonances I_{1B}^1 and I_{1B}^2 clear up this situation. In a field $\mathbf{H}\perp\mathbf{c}$ both resonances show a threefold split-off. This contradicts the assumption that these lines represent transitions only into the lower Γ_9 state of the (A^0,X_B) complex, a state which is not allowed to split in $\mathbf{H}\perp\mathbf{c}$ (compare the term scheme in Fig. 5). Thus we state that the threefold splitting of both resonances in a field $\mathbf{H}\perp\mathbf{c}$ is due to the mixing of the two closely neighboring Γ_9 and Γ_8 levels of the (A^0,X_B) complex as it is predicted by

theory (see Sec. IV B).

Thus the $\Gamma_3 \oplus \Gamma_4$ state originating from the lower Γ_9 level lies between Γ_3 and Γ_4 originating from the Γ_8 level and not below them as it has been suggested by Fig. 5. In $\mathbf{H} \perp \mathbf{c}$, all transitions to states which originate from these two zero-field levels are allowed with a polarization $\mathbf{E} \| \mathbf{c}$, in agreement with the experimental observations.

The splitting between the two outer lines of each Zeeman triplet yields a g value which amounts to 3.2 and 3.42 for I^1_{1B} and I^2_{1B}, respectively. Since the acceptor A^0 is a pure Γ_9 state its splitting obeys Eq. (8) and is zero for $\mathbf{H} \perp \mathbf{c}$. Thus, the experimental g values are directly the values $g_{3,\perp}$ of the bound-exciton levels which occur in Eq. (10). Additionally, the excitation resonances I^1_{1B} and I^2_{1B} should not show any thermalization effect. In fact the two outer components of both triplets are equal in strength. The respective middle lines are stronger. This can be explained by their larger transition probability due to the strong contribution of the Γ_9 levels.

(b) $\mathbf{H} \| \mathbf{c}$. I^1_{1B} and I^2_{1B} show a twofold splitting both with $g = 2.96$ and the low-energy component being stronger in intensity (see Table II). This indicates that the A^0 state is also split, but the upper level, i.e., the $\Gamma_9(A^0,X_B)$-level splitting is larger. These results agree with theory which predicts no mixing of states for the case $\mathbf{H} \| \mathbf{c}$ and a twofold split of the Γ_9 states. For reason of the usual momenta selection rules only two transitions are allowed, one between the lower A^0 component to the lower (A^0,X_B) component and the other between the respective upper components. Thus following Eq. (8) the value $g_{2,\|}$ of the lower Γ_9 state in the (A^0,X_B) term scheme can be determined from the $I^{1,2}_{1B}$ split off in a field $\mathbf{H} \| \mathbf{c}$. From the experiment and with the known acceptor g value $g(A^0) = -2.7$ (Ref. 13) there results a $g_{2,\|} = -5.66$.

In fields of more than 5 T an additional twofold structure occurs between the I^2_{1B} doublets. These lines can be interpreted as the split-off components of the nearly neighboring $\Gamma_9(A^0) \leftrightarrow \Gamma_8(A^0,X_B)$ transition which is dipole forbidden in the zero-field case as well as in a field $\mathbf{H} \| \mathbf{c}$, which has been shown by means of group theory (Sec. IV A). But the high excitation densities used in our measurements make possible a significant amount of quadrupole transitions as is also observable in the case of other dipole forbidden bound-exciton transitions.[1,3,4] The g value of the $\Gamma_8(A^0,X_B)$ state is calculated from the splitting of these additional structures to be about $g_{1,\|} = -3.7$.

2. *The transitions $I^1_{1B'}$ and $I^2_{1B'}$*

The situation becomes more complicated for the lines $I^1_{1B'}$ and $I^2_{1B'}$. Both lines are broader and weaker than I^1_{1B} and I^2_{1B} so that the overlap of the lines hinders the clear observation especially of weak components.

(a) $\mathbf{H} \perp \mathbf{c}$. The splitting of both lines should be described by Eq. (10) with a value $g'_{3,\perp}$. However, only two components can be seen in the spectra being equal in strength. $I^2_{1B'}$ exhibits a $g'_{3,\perp} = 2.05$. For $I^1_{1B'}$ the high-energy component seems to be totally superimposed by the strong lines which originate from I^2_{1B}.

(b) $\mathbf{H} \| \mathbf{c}$. Both lines $I^1_{1B'}$ and $I^2_{1B'}$ show only a high-energy component. According to the theory these lines should split into a doublet but should exhibit strong thermalization effects so that a low-energy component is hardly to be expected at 1.6 K. If the experimentally observed lines are regarded as being the high-energy components of both doublets it is possible to determine a g value from their course, which is given in Table II. The momenta selection rules are valid in the same sense as for the case of I^1_{1B} and I^2_{1B}. From that with regard to the thermalization, a $g'_{2,\|} = -0.8$ is estimated for the upper Γ_9 levels of the (A^0,X_B) complex.

3. *g values of the particles*

The calculated g values of the (A^0,X_B) levels are given in Table V. From these data several g values of the particles involved can be calculated. The anisotropic g values of the A and B holes enter into Eqs. (11) and (12) which describe the splitting of the Γ_9 states in a field $\mathbf{H} \| \mathbf{c}$. With the experimental g values of these transitions and with an isotropic electron g value of $g_e = -1.78$ (Refs. 5 and 13), one yields a completely anisotropic g value of the A hole, $g_{hA} = -3.23$. $g_{hB\|}$ amounts to -4.22 within the Γ_9 states.

The experimental values determined for the Γ_8 level are $g_\perp = -3.42$ and $g_\| = 3.7$. This is consistent with theory expecting a nearly isotropic behavior of the Γ_8 and Γ_7 levels of the (A^0,X_B) complex.

The g value of the A hole $g_{hA} = -3.23$ supports the assumption that the properties of the A hole are very sensitive to its state of binding. Whereas the free A hole shows a g value of -1.25,[31,32] it has a $g = -1.8$ in the (D^0,X) complex,[5] a $g = -2.7$ to -2.76 in the acceptor A^0,[13,33] and the now determined $g = -3.23$ in the (A^0,X_B) complex.

In Sec. IV B it was pointed out that the zero-field splitting between the lower Γ_9 and the Γ_8 state on the one hand and the upper Γ_9 and the Γ_7 state on the other hand should be smaller than 40 μeV. This supports the assumption that the electron-hole exchange interaction is too weak to allow a direct observation of the energy shift caused by this interaction in the zero-field case. However, the investigation in the magnetic field offers an excellent possibility of resolving all (A^0,X_B) transitions by their different splitting behavior.

In fact the experimental spectra in the zero-field case $\mathbf{H} = \mathbf{0}$ show no resolvable doublet structures within the experimental resolution of 0.01 nm.

TABLE V. Calculated g values for the (A^0,X_B) states.

State	$\mathbf{H} \perp \mathbf{c}$	$\mathbf{H} \| \mathbf{c}$
$\Gamma_9(I_{1B})$	-3.42	-5.66
Γ_8		-3.7
Γ_7	-2.05	Not seen
$\Gamma_9(I_{1B'})$		-0.8

V. SUMMARY AND CONCLUSIONS

By means of excitation spectroscopy of the I_1 luminescence due to the (A^0,X_A) recombination, we were able to develop a self-contained model of the electronic ground state of the (A^0,X_B) complex, including all fine-structure effects due to the interparticle interactions involved. This made possible the elucidation of a number of undigest experimental effects and of misinterpretations given before. So the ratio between the hole-hole and the electron-hole exchange interactions could be satisfactorily explained in agreement with the experimental findings. It was shown that the electron-hole exchange interaction only yields to very small energy distances between the affected states. Nevertheless, the investigation in a magnetic field gives an excellent possibility of establishing the electronic and symmetry properties of each of the states split off by the electron-hole-exchange interaction. The results allow the development of a complete term scheme of the (A^0,X_B) complex and the assignment of all experimentally observed transitions to the levels within the scheme. For the states involved the g values could be determined. From these results g values of the particles within the complex are calculated. The influence of chemical effects on the binding energies of (A^0,X) complexes could be shown to be more complicated than it has been assumed in theoretical treatments up to now. Especially, the binding energy does not depend monotonously on the effective mass ratios of the particles involved as it has been predicted before. Thus the (A^0,X_A) configuration is not affected in the same way by a change of the acceptor center as it is the (A^0,X_B) complex.

Our results should help to improve the treatment of ground and excited states of bound excitons. The knowledge of these states is important because transitions into these levels give rise to high-density effects such as forbidden transitions and electronic Raman scattering[22] within bound excitons and interact with pure high-density effects, like the biexciton creation and exciton-exciton scattering processes. Thus they offer further knowledge on the excitation and recombination mechanisms in the exciton region of semiconductor compounds.

ACKNOWLEDGMENTS

The author wishes to thank Dr. R. Broser (Fritz-Haber-Institut) for supplying the crystals, Professor I. Broser for helpful discussions, and H. Perls and T. Hönig for technical assistance performing the measurements in a magnetic field. The magnet was financed by the Deutsche Forschungsgemeinschaft.

[1]R. Baumert, I. Broser, J. Gutowski, and A. Hoffmann, Phys. Rev. B **27**, 6263 (1983).
[2]R. Baumert, I. Broser, J. Gutowski, and A. Hoffmann, Phys. Status Solidi B **116**, 261 (1983).
[3]J. Puls and J. Voigt, Phys. Status Solidi B **94**, 199 (1979); J. Puls, I. Rückmann, and J. Voigt, *ibid.* **96**, 641 (1979); J. Puls, H. Redlin, and J. Voigt, *ibid.* **107**, K71 (1981).
[4]J. Puls, F. Henneberger, and J. Voigt, Phys. Status Solidi B **119**, 291 (1983).
[5]A. Roussel, diplomathesis, Institut für Festkörperphysik, Technische Universität, Berlin, 1979.
[6]C. H. Henry and K. Nassau, Phys. Rev. B **2**, 977 (1970).
[7]H. Malm and R. R. Haering, Can. J. Phys. **49**, 2432 (1971).
[8]O. Goede, M. Blaschke, and U. H. Klohs, Phys. Status Solidi B **76**, 267 (1976).
[9]R. Baumert and J. Gutowski, Phys. Status Solidi B **107**, 707 (1981).
[10]C. Klingshirn, W. Maier, G. Blattner, P. J. Dean, and G. Kobbe, J. Cryst. Growth **59**, 352 (1982).
[11]G. Schmieder, W. Maier, Liu Pu-Lin, and C. Klingshirn, J. Lumin. **28**, 357 (1983).
[12]Le Si Dang, A. Nahmani, and R. Romestain, Solid State Commun. **46**, 743 (1983).
[13]D. G. Thomas and J. J. Hopfield, Phys. Rev. **128**, 2135 (1962).
[14]V. M. Edelstein, Solid State Commun. **23**, 499 (1977).
[15]D. C. Herbert, J. Phys. C **10**, 3327 (1977).
[16]B. Stébé and G. Munschy, Solid State Commun. **35**, 557 (1980); **40**, 663 (1981); **43**, 841 (1982).
[17]D. S. Pan, Solid State Commun. **37**, 375 (1981).
[18]W. Ungier and M. Suffczynski, Phys. Rev. B **27**, 3656 (1983).
[19]D. G. Thomas, R. Dingle, and J. D. Cuthbert, in *Proceedings of the Seventh International Conference on II-VI Semiconducting Compounds, Providence, R.I.,* edited by D. G. Thomas (Benjamin, New York, 1967), p. 863.
[20]C. H. Henry, K. Nassau, and J. W. Shiever, Phys. Rev. B **4**, 2453 (1971).
[21]J. J. Hopfield and D. G. Thomas, Phys. Rev. **122**, 35 (1961).
[22]J. Gutowski and I. Broser, following paper, Phys. Rev. B **31**, 3621 (1985).
[23]T. Hönig and J. Gutowski, presentation at the 5th General Conference of the Condensed Matter Division of the European Physical Society, Berlin, Germany, 1985 (unpublished).
[24]I. Broser, J. Gutowski, and R. Riedel, Solid State Commun. **49**, 445 (1984).
[25]G. F. Koster, J. O. Dimmock, R. G. Wheeler, and H. Statz, *Properties of the Thirty-Two Point Groups* (M.I.T. Press, Cambridge, Mass., 1963).
[26]W. Ungier, M. Suffczynski, and J. Adamowski, Phys. Rev. B **24**, 2109 (1981).
[27]E. I. Rashba, Fiz. Tekh. Poluprovodn. **8**, 1241 (1974) [Sov. Phys.—Semicond. **8**, 807 (1975)].
[28]J. C. van den Bosch, in *Spectroscopy II,* Vol. 28 of *Encyclopedia of Physics,* edited by S. Flügge (Springer, Berlin, 1957), p. 296.
[29]V. V. Sobolev, V. I. Donetskina, and E. F. Zagainov, Fiz. Tekh. Poluprovodn. **12**, 1089 (1978) [Sov. Phys.—Semicond. **12**, 646 (1978)].
[30]B. Stébé and G. Munschy, Phys. Status Solidi B **88**, 713 (1978).
[31]H. Venghaus, S. Suga, and K. Cho, Phys. Rev. B **16**, 4419 (1977).
[32]I. Broser and M. Rosenzweig, Phys. Rev. B **22**, 2000 (1980).
[33]C. H. Henry, R. A. Faulkner, and K. Nassau, Phys. Rev. **183**, 798 (1969).